Estimating Albedo of Specular Objects

Diego THOMAS† and Akihiro SUGIMOTO†

† National Institute of Informatics, Chiyoda, Tokyo
E-mail: †{diego.thomas,sugimoto}@nii.ac.jp

Abstract We present a method for estimating albedo of a specular object from its range images acquired under unknown single or multiple light sources. Our method retrieves information on incident illumination from specular highlights to locally separate reflection components at the surface. We first discriminate between specular highlights and high intensity texture regions using illumination consistency on two range images. We then estimate light sources directions from specular highlights. With different light source directions, we then indentify regions where diffuse reflection components can be extracted. By using estimates of light source directions and the diffuse reflection components, we locally compute albedo at the surface. Albedo is then extrapolated into the overall surface. This technique can handle various kind of illumination situations and can be applied to a wide range of materials. Our experiments using synthetic data and real data show the effectiveness, the robustness and the accuracy of our proposed method.

1. Introduction

Accurate and reliable estimation of point correspondences in two overlapping 3D images has been of crucial interest in the past decades. Such correspondences are widely used in applications such as registration or camera calibration for example. Estimating point correspondences between two images can be decomposed into two parts: (1) extracting reliable and discriminative features and (2) defining a similarity measure to match points.

Range images are a special case of 3D images, and they are widely used for creating detailed 3D models of real objects. The latest laser scanning technologies enable the accurate acquisition of both geometry and color information from the object of interest. In this paper, we will focus on extracting reliable and discriminative features from two range images of a non-Lambertian textured surface devoid of salient geometric features even without a priori knowledge on incident illumination. Such a situation is challenging in that (1) geometric features are not discriminative enough for point correspondences estimation, (2) non-Lambertian surfaces present both diffuse and specular reflections and (3) the incident illumination composed of a single or multiple distant light sources with arbitrary color is unknown (hereafter, we will refer to such illumination as uncontrolled illumination). Note that outdoor situations are not comsidered in this paper; illumination is thus assumed to be fixed. We assume that two range images in different poses are captured from a fixed viewpoint under fixed and uncontrolled illumination. We also assume that there are no shadows nor inter-reflections.

The irradiance at a point on an object surface changes when the object pose changes. As a consequence, the photometric appearance, such as color, of the same point in different range images changes. Using photometric features that depend on the object pose thus degrades the performance of estimating point correspondences.

On the other hand, albedo is the ratio of the diffuse reflected light over the irradiance, and it is well known as an invariant feature to the object pose, viewpoint or illumination. It depends on only the object material and exhibits sufficient saliency for the point correspondence problem in the case of textured surfaces.

Albedo at a point can be directly estimated when both the diffuse reflection and the incident illumination at this point are known. However, under uncontrolled illumination or if the surface exhibits specular reflections (like a shiny surface for example), computing albedo becomes a demanding problem. As a consequence, previous work on estimating albedo ([2] for example) assumes the diffuse reflection model, and existing matching techniques ([4], [15] for example) that make use of albedo are thus also limited to Lambertian surfaces.

We propose a method for extracting albedo from two range images of a specular object under fixed and uncontrolled illumination even in the presence of high in-

tensity texture. To compute albedo at the surface, incident illumination and diffuse reflection components are required. For each range image, we generate candidates of light source directions, using normals at the surface and local peak of intensity. Illumination consistency on two range images allows us to select light source directions among the candidates. The detected light source directions then enable us to define regions where the reflection components are accurately separated. We compute albedo in these regions and extrapolate it by using neighboring similarities. In this way, we obtain albedo over the range images. Fig. 1 illustrates the flowchart of our proposed method. Our intensive experiments show the effectiveness of our proposed method. The contributions of this paper are (1) an efficient technique to discriminate between specular highlights and high intensity texture regions; (2) identification of regions where the reflection components can be separated even under uncontrolled illumination and (3) an extrapolation technique to maximize the amount of points with estimated albedo. These contributions result in robust and accurate extraction of albedo in practical situations.

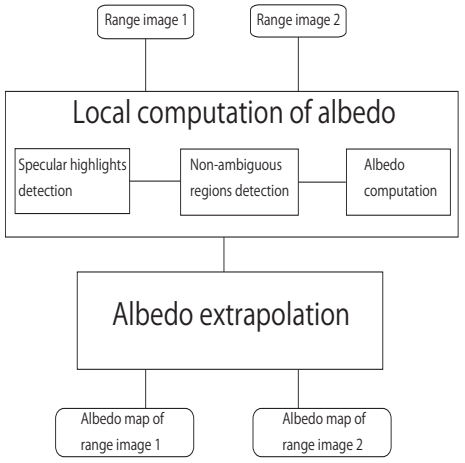

Fig. 1 Basic flow of the proposed method.

2. Related work

For objects lacking in salient geometric features, many photometric features have been discussed to solve the 3D point correspondence problem. For example, Okatani *et al.* [9] proposed to use chromaticity. Brusco *et al.* [3] proposed to incorporate texture information in the concept of spin-images. Pulli *et al.* [10] proposed a new mismatch error using both color and geometric information. However, because color or chromaticity depends on the object pose, the viewpoint and illumination, the reliability of these features is degraded when the illumination change has significant effects on the object appearance. More recently, Shinozaki *et al.* [12] proposed a method for correcting color information of a 3D model using range intensity images. However, a range intensity image contains a reflectance image which requires heavy experimental set up and this method can not be used without a priori knowledge on incident illumination.

On the other hand, albedo at the surface of an object is a photometric property invariant to the pose of the object, the illumination condition and the viewpoint, and is thus powerful for the purpose of matching ([4], [15]). Biswas *et al.* [2] recently proposed a method for robustly estimating albedo from a single image illuminated by a single or multiple light sources, using the errors statistics of surface normals and illumination direction. However, this method assumes the diffuse reflection model and is thus limited to Lambertian surfaces.

To deal with specular reflections under uncontrolled illumination, recent works on reflectance analysis can be used. Several methods to separate or decompose reflection components of textured surfaces can be found in the literature ([7], [11], [6]). For example, Lin *et al.* [6] proposed to separate reflection components from a sequence of images by computing the median intensity of corresponding pixels in the image sequence. However, this method requires a large number of images as well as pixel correspondences over all images. It is thus inappropriate in our situation.

Tan *et al.* [13] proposed a method to separate reflection components of textured surfaces from a single image. By assuming the dichromatic reflection and a single distant light source, a specular free image is generated by locally and non-linearly shifting each pixel's intensity and maximum chromaticity. This specular free image has exactly the same geometrical profile as the diffuse components. Though this method achieves accurate separation of reflection components, it can not handle multiple light sources and high intensity textures. Thus, it can not be directly applied in our situation.

In contrast to previous work, our proposed method has the advantage for non-Lambertian objects under uncontrolled illumination even in the presence of high intensity texture regions.

3. Local estimation of albedo

Computing albedo at the surface requires the diffuse reflection components and the light source directions. In the case of a scene illuminated by a single distant light source and given the corresponding illumination

chromaticity, a method exists that separates the reflection components of the textured surface [13]. On the other hand, in our case, the incident illumination is not restricted to a single light source and such a separation technique can not be applied to the whole surface. However, even in the case of multiple light sources, there exist some regions where the incident illumination can be approximated by a single light source. We thus divide the whole image into regions so that we have a region that is approximated by a single light source illumination. We call such a region non-ambiguous. We can then separate reflection components of non-ambiguous region to locally compute albedo.

3.1 Detection of specular highlights

For a smooth surface, a specular highlight is centered on the mirror-like reflection direction, which is useful to estimate incident illumination direction. The specular highlights are also useful to estimate the illumination chromaticity. However, if the surface exhibits regions with high intensity texture, it becomes difficult to distinguish between specular highlights and regions with high intensity texture. Therefore, we first detect all highlights at the surface that can be either a specular highlight or a high intensity texture region. We then employ illumination consistency between two range images to discriminate specular highlights from high intensity texture regions.

3.1.1 Highlight detection

Specular highlights exhibit local peaks of intensity at the surface of a specular object. This is because the specular reflection component increases as the viewing direction comes closer to the mirror-like reflection direction, while the diffuse component remains locally stable.

Starting the detection with the whole surface as a single connected region, we iterate the following process to obtain highlights regions at the surface. For each connected region, the average avg and standard deviation std of the intensities are computed, and each pixel $\mathbf{x}$ such that $\mathbf{I}(\mathbf{x}) > avg + std$ is selected, where $\mathbf{I}(\mathbf{x})$ is the intensity at $\mathbf{x}$. Then, if the initial connected region is separated into several connected parts, the same process is applied to each connected part. The detection stops when the number of connected regions becomes stable. Each connected region represents one possible specular highlight.

3.1.2 Specular highlights

Some of the detected highlights may be high intensity texture regions, which may cause false detection of incident illumination. We first compute light source direction of each highlight and then employ illumination consistency to discriminate between specular highlights and high intensity texture regions.

The illumination condition is assumed to be fixed. This means that the light source directions producing corresponding specular highlights are the same. We will call this illumination consistency.

Normals at the surface are available for two range images. We can thus estimate the incident illumination direction that can produce such highlight, for each highlight in two range images. To be more specific, we compute the average of the incident light vectors in the highlight region, where an incident light vector at a point $\mathbf{x}$ is computed by rotating the viewing direction at point $\mathbf{x}$ around the normal at point $\mathbf{x}$ with an angle of $\frac{\pi}{2}$. This is because for smooth surfaces, the viewing directions in this region are roughly centered on the mirror-like specular reflection direction.

The highlight regions are then clustered into groups that are produced by similar light sources. Namely, consider the sets $(H_{1,j})_{j\in[0,n_1]}$ and $(H_{2,j})_{j\in[0,n2]}$ of the highlight regions of two range images, with n_1 and n_2 the number of highlight regions in the two range images respectively. We regroup highlight regions using the criterion below:

$$\forall i \in [1,2], \forall (j,j') \in [0,n_i], \text{ if } \mathrm{acos}(\mathbf{l}_{\mathrm{i,j}} \cdot \mathbf{l}_{\mathrm{i,j'}}) < \mathrm{Th_l}$$
$$\text{then the corresponding regions are combined,}$$

where $\mathbf{l}_{i,j}$ is the estimated normalized light direction for the highlight region $H_{i,j}$, $(\mathbf{l} \cdot \mathbf{l}')$ is the scalar product of two vectors $\mathbf{l}$ and $\mathbf{l}'$, and Th_l is a threshold (for example 20 degrees). When two regions $H_{i,j}$ and $H_{i,j'}$ are combined into a group, $H_{i,j'}$ is added to $H_{i.j}$, $l_{i,j} = \frac{l_{i,j}+l_{i,j'}}{2}$and $H_{i,j'}$ is removed from the list of highlight regions.

We then eliminate high intensity texture regions using the illumination consistency constraint. Namely, we use the criterion below:

$$\forall i \in [1,2], \forall j \in [0,n_i], \text{if } \forall i' \in [1,2], i' \neq i, \forall j' \in [0,n_{i'}],$$
$$\mathrm{acos}(\mathbf{l}_{\mathrm{i,j}} \cdot \mathbf{l}_{\mathrm{i',j'}}) > \mathrm{Th_l},$$
$$\text{then the region } H_{i,j} \text{is eliminated.}$$

Figure 2 illustrates the illumination consistency constraint under a fixed viewpoint and fixed illumination condition.

We finally obtain consistent specular highlights on two range images with their estimated incident light direction. These specular highlights are also used to compute the illumination chromaticity of each light source. The estimated light source directions are used to detect

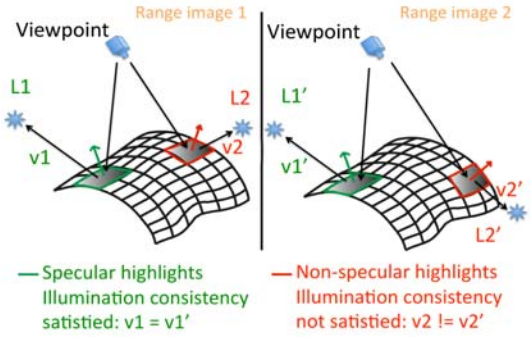

Fig. 2 Illumination consistency constraint.

non-ambiguous regions each of which is mostly illuminated by a single dominant light source. Detail of these procedures will be given in the next sections.

3.2 Detection of non-ambiguous regions

For each specular highlight, we have estimated its mostly dominant light source direction. If the incident illumination of a region is a single distant light source, we can use the method [13]. We can not, however, directly apply the method [13] to the whole surface, because the incident illumination can be composed of multiple light sources. We thus detect from the surface non-ambiguous regions where the local incident illumination can be approximated by a single distant light source.

We assume that each detected light source is distant from the surface so that the incident light rays coming from one light source are the same for all points over the surface. By using the detected incident light directions, we compute a shadow map for each detected light source. Namely, for a light L with directional vector $\mathbf{l} = (l_x, l_y, l_z)$, we define the shadow map S induced by L proportional to the energy received from L by each point at the surface. More precisely, for a point $\mathbf{x}$ on the surface with normal $\mathbf{n}$ and with angle Θ between $\mathbf{l}$ and $\mathbf{n}$, we define

$$S(\mathbf{x}, L) = \cos\Theta.$$

To detect non-ambiguous regions, we use the criterion below:

$$\text{if } |S(\mathbf{x}, L_1) - S(\mathbf{x}, L_2)| > Th_\alpha$$

$$\text{then } \mathbf{x} \text{ is in a non-ambiguous region}$$

$$\text{else } \mathbf{x} \text{ is in an ambiguous region,}$$

where L_1 and L_2 are the two light sources such that the intensities of the shadow maps at the point $\mathbf{x}$ are the greatest. The threshold Th_α is a value between 0 and 1. In the experiments, we chose $Th_\alpha = 0.4$ that corresponds to an angle Θ of about 20 degrees. For each non-ambiguous regions, we attach the light source that emits the most energy inside this region and regroup regions with the same corresponding light sources. We remark that it is preferable to under-detect non-ambiguous regions rather than ambiguous regions. This is because high errors in albedo estimations in non-ambiguous regions may propagate during the subsequent extrapolation process.

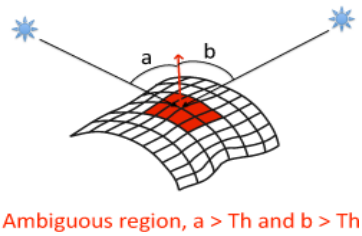

Fig. 3 Definition of ambiguous regions.

As a consequence, we obtain non-ambiguous regions in two range images in which we can reliably and adaptively separate reflection components using a single distant light source.

3.3 Estimating albedo in non-ambiguous regions

For each non-ambiguous region, the incident illumination can be approximated by a distant single light source whose illumination chromaticity can be estimated. We can thus independently apply the method proposed in [13] to each non-ambiguous regions for separating the reflection components of these parts of the surface. We briefly recall the method proposed in [13].

The dichromatic reflection model at a pixel $\mathbf{x}$ can be expressed as:

$$\mathbf{I}(\mathbf{x}) = \omega_d(\mathbf{x})\mathbf{B}(\mathbf{x}) + \omega_s(\mathbf{x})\mathbf{G}(\mathbf{x}), \qquad (1)$$

where $\mathbf{I} = (I_r, I_g, I_b)$ is the color vector of image intensity, $\mathbf{x} = (x, y)$ is the image coordinate, $\omega_d(\mathbf{x})$ and $\omega_s(\mathbf{x})$ are the weighting factors for diffuse and specular reflections, $\mathbf{B}(\mathbf{x})$ represents the color vector of diffuse reflection and $\mathbf{G}(\mathbf{x})$ represents the color vector of the specular reflection. Note that we assume that the specular reflection intensity is equal to the illumination intensity, without any inter-reflections. The first part of the right-hand side in (1) represents the diffuse reflection component and the second part represents the specular reflection component. The basic idea for separating reflection components is to iteratively compare the intensity logarithmic differentiation of an input image and its specular-free image. We remark that a specular-free image is an image that has exactly the same profile as the diffuse image.

The input image should be a normalized image that simulates a pure white illumination. Accordingly, the input image is normalized by the illumination chromaticity. To compute illumination chromaticity, several methods based on color constancy can be found in the literature([14], [5] for example). In particular, the method [14] achieves robustness as well as accurate estimation of the illumination chromaticity by using specular reflection intensity. The specular-free image is generated by shifting each pixel's intensity and maximum chromaticity nonlinearly. Given a normalized and a specular-free image, the reflection components are then iteratively separated until the normalized image has only diffuse pixels.

As a result, a diffuse normalized image is obtained. This estimated diffuse image is then used, together with the estimated light source direction corresponding to the non-ambiguous region and the diffuse reflection model, to estimate albedo in this region.

4. Extrapolation of albedo into ambiguous regions

Up to here, we have computed albedo in non-ambiguous regions. However, in ambiguous regions, albedo is still unknown and matching points in these regions is not yet possible. We estimate albedo in the ambiguous region by extrapolating albedo computed in non-ambiguous regions.

We consider a small region at the surface without specular highlights. The energy reflected at points inside this region is then mostly diffuse. As a consequence, the chromaticity σ of points inside this region with the same surface color is similar to each other. Therefore, comparing chromaticity of points inside the regions allows us to detect points with similar albedo.

Starting from diffuse points in the ambiguous region that have a neighbor in a non-ambiguous region, albedo values are iteratively and locally extrapolated until the size of the ambiguous region converges to a constant value. At each iteration, considering a point $\mathbf{x}$ at the border of the ambiguous region, we extract the point $\mathbf{y}$ in the neighborhood of $\mathbf{x}$ such that $\epsilon = |\sigma(\mathbf{x}) - \sigma(\mathbf{y})|$ is minimal and albedo of $\mathbf{y}$ is known. If ϵ is smaller than a threshold Th_ϵ (for example $Th_\epsilon = 0.1$), then we set the albedo value of $\mathbf{x}$ to that of $\mathbf{y}$, and remove $\mathbf{x}$ from the ambiguous region. Namely, we process as follows:

$$\mathbf{y} = \text{argmin}_{\mathbf{p}\in V(\mathbf{x})}(|\sigma(\mathbf{x}) - \sigma(\mathbf{p})|),$$

$$\text{if } |\sigma(\mathbf{x}) - \sigma(\mathbf{y})| < Th_\epsilon, \text{then } alb(\mathbf{x}) = alb(\mathbf{y})$$

and we remove $\mathbf{x}$ from the ambiguous region,

where $alb(\mathbf{x})$ is the albedo of point $\mathbf{x}$ and $V(\mathbf{x})$ is a neighborhood of $\mathbf{x}$ such that $\forall \mathbf{p} \in V(\mathbf{x}), \|\mathbf{x} - \mathbf{p}\|_2 < Th_V$ and $\mathbf{p}$ is in a non-ambiguous region, with Th_V a threshold (for example $Th_V = 0.06$ mm if the resolution of range image is 0.01 mm). Fig. 4 illustrates the extrapolation procedure.

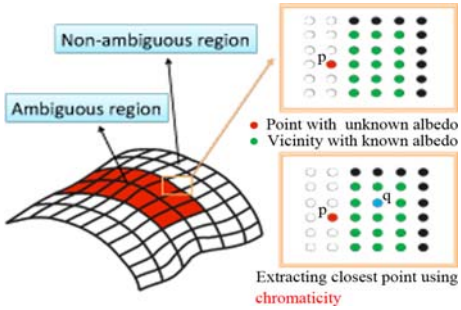

Fig. 4 Extrapolation into ambiguous regions.

As a result, we extrapolate albedo to the rest of points at the surface that are not inside a specular highlight.

5. Experiments

In order to show the usefulness of our method, we use our estimated albedo image as an input of the recently proposed range image registration method [15]. The method [15] uses adaptive regions defined from the local distribution of albedo. A similarity metric between two points of interest is then defined based on the albedo similarity of corresponding points inside the regions weighted by the geometric similarity of the regions.

Because objects used in our experiments have a shape devoid of salient geometric properties, the registration using only geometric characteristics does not work well. As a consequence, the standard RMS using point-to-point Euclidean distance errors is not relevant to evaluate the registration results in our case. In this paper, we evaluate registration results by comparing the obtained transformation with the ground truth transformation.

We use an angular measure of errors for the rotation like in [1], and the standard Euclidean error for the translation. Let (R_g, T_g) be the ground truth transformation and (R_e, T_e) be the estimated transformation, with R_g, R_e the rotations and T_g, T_e the translations. A rotation $R = \cos(\frac{\alpha}{2}) + \overrightarrow{u}\sin(\frac{\alpha}{2})$ is represented using the quaternions, where α is the angle of the rotation and $\overrightarrow{u}$ is the unit vector representing the rotation axis. Let res be the resolution and d the depth of range images, we define err, the error of the obtained transformation, by

$$err = \frac{\Theta d + ||T_g - T_e||}{res}, \qquad (2)$$

where Θ is the angle between the normalized ground truth rotation $\frac{R_g}{||R_g||}$ and the normalized estimated rotation $\frac{R_e}{||R_e||}$. We remark that the unit of *err* is the resolution of range images. It is thus an objective and informative criterion to evaluate the accuracy of the different registration methods. In these experiments, all results are shown with estimated albedo images.

5. 1 Evaluation with synthetic data

We conducted experiments with synthetic data to evaluate the robustness of our proposed method against changes in illumination conditions and noise in both normals and intensities. The synthetic data were obtained with a 3D modeler software (3D Studio Max), each range image had about 30000 points with a resolution of 0.01 mm. The exact albedo image is known. We simulated intensity at the surface with a known specular reflection component and synthetic light sources using the Torrance and Sparrow reflection model [8].

Before applying our method, we manually established a rough pre-alignment of two range images. This alignment allowed us to simulate the case where the input data were captured from two different viewpoints rotationally differentiated by 18.00 degrees around the axis $(0.006, 0.999, -0.026)$ and with a translation of $(-0.02, 0.00, -0.01)$.

In order to see the effects against data noise, we randomly transformed the normals and intensity of the two range images. More precisely, let the latitude and longitude angles between the direction of the perturbed normal and the ground truth normal be (α, ϕ), in which ϕ is a number uniformly generated from 0 degree to 360 degrees. The normals were perturbed with different values of α. On the other hand, the surface intensity was perturbed with Gaussian noise with 0 mean and λ variance, where λ is a percentage of the average over the ground truth intensity of the surface.

We evaluated our method with different values of α and λ. The value α was changed from 0 to 7 degrees by 0.6 degrees. The value λ was changed from 0 to 5 percents by 0.25 percents. For each values of α, λ, we applied our method 50 times under the same initial conditions.

Figure. 5 shows quantitative evaluation of registration results under various different level of noise in both normals and in intensity. Our method achieves robustness for both noise in normals and intensity. We observe that even with a noise in intensity of variance 5%, the largest error remains under 0.5 times the resolution of the image. For noise in normals, we observe that even with a noise of variance 7 degrees, the largest error remains under 1.0 times the resolution of the image. Fig. 6 shows an example of the input range images and the estimated albedo. In this example, we obtained and error of 0.2 times the resolution of the image. We observe that the registration achieves accuracy of the same precision of the acquisition device accuracy. We also observe that as expected, the specular effects are correctly removed and that the features are globally invariant to the viewpoint, the pose of the object and the illumination. Moreover, the obtained albedo is consistent for the two range images.

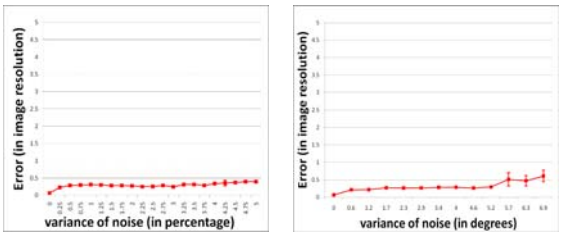

(a) Noise in intensities. (b) Noise in normals.

Fig. 5 Results under various noise.

(a) (b) (c) (d)

Fig. 6 The input synthetic data and estimated albedo images. (a) input image 1 and (b) its estimated albedo image. (c) input image 2 and (d) its estimated albedo image.

In order to see the effects against illumination conditions, we rendered two images with various kinds of illumination. The light source direction is computed using the normal at a point $\mathbf{x}$ and the viewpoint, and the light source position is defined at an arbitrary distance on the light direction. This is because we need specular highlights at the surface and we prefer to choose a random point $\mathbf{x}$ at the surface that represents the perfect specular reflection from the viewpoint, rather than choosing the position of the light source randomly.

We changed the position between the specular highlights that define the light source directions. One light was fixed and considered as a reference light. We then evaluated our method with three different values of d,

where d is the distance of two different specular highlights: 1.2, 1.0 and 0.8. For each value of d, our method was applied 50 times with a random light direction. Table 1 shows the results obtained with our method. The value *Ratio* is the ratio of ambiguous points over the total number of points in the two range images. We observe that the largest error remains under 1.0 time the resolution of the image. Figs. 7 illustrates the estimated albedo obtained with our method when using two light sources with $d = 1.0$. For comparison, the result obtained with the method proposed in [15] is also shown. The method [15] had an error of 24.827 times the resolution of the image. In contrast, our method obtained accurate result, with an error of 0.244 times the resolution of the image. We observe that the ratio of ambiguous points was of 0.393 in this experiment.

(a) (b) (c) (d)

Fig. 7 Simulation with two light sources. (a) input image; (b) our albedo image in non-ambiguous regions; (c) our obtained albedo image; (d) albedo image using the diffuse reflection model.

Tbl. 1 Results obtained with two light sources.

d	Error	Variance of Error	Ratio	Variance of ratio
1.2	0.886	0.194	0.445	0.041
1.0	0.315	0.022	0.406	0.066
0.8	0.467	0.088	0.354	0.048

5. 2 Evaluation with real data

We also conducted experiments using real data. We evaluated our method by comparing with registration results obtained using the albedo image computed with the diffuse reflectance method. We also compared with registration results obtained using chromaticity. We selected these two comparison methods for the reasons below.

- To our best knowledge, existing methods that make use of albedo for registering overlapping range images (like proposed in [4] and [15] for example) approximate the reflection model with the diffuse reflection model. This approximation is relevant for many types of objects when the viewpoint is far from the mirror-like reflection direction. It is thus often useful to compute albedo for registering overlapping range images.
- Chromaticity is tolerant to some extent against changes in illumination. Using chromaticity for registering overlapping range images is, therefore, more reliable than using brightness of the object.

We employed a Konica Minolta Vivid 910 range scanner, which captures the 3D shape and the texture of an object. A mechanic system was used for object rotations. Because the position and orientation of the range scanner are unknown, it is difficult to obtain the ground truth from the experimental setup. In order to obtain the ground truth, we manually chose about 10 corresponding points in two range images and computed the transformation that minimizes the distance between each corresponding points. We used this ground truth to evaluate errors using equation (2). We note that for this experiments we took care not to have saturated pixels and to remove the gamma correction of the camera.

We obtained to range images of a sphere with specular reflection components under fixed and uncontrolled illumination (Fig. 8). Fig. 8 shows estimated albedo images. Each range image had about 31000 points with a resolution of 0.53 mm. The ground truth transformation is shown in Table 2. The results obtained with three methods are shown in Fig. 9. The quantitative results of the registration by the three methods are shown in Table 3.

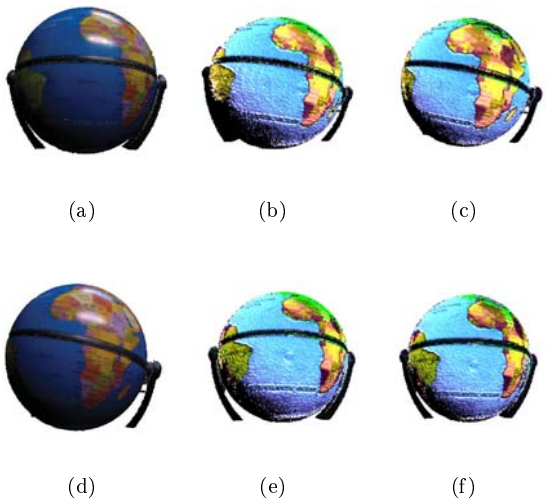

(a) (b) (c)

(d) (e) (f)

Fig. 8 The data *globe*. Input image 1 (a), albedo of image 1 in non-ambiguous regions (b) and after extrapolation (c). Input image 2 (d), albedo of image 2 in non-ambiguous regions (e) and after extrapolation (f). Ambiguous regions are displayed in vivid green.

(a) (b) (c)

Fig. 9 Results obtained with different methods. (a) our method; (b) using diffuse reflection model; (c) using chromaticity.

Tbl. 2 The ground truth transformation for data *globe*.

Exp_Rotation	Expected_Translation
(22.49, 0.02, 0.94, 0.33)	(9.32, 0.12, −1.54)

Tbl. 3 Results obtained for the data *globe*.

Error	Rotation	Translation
Proposed method		
0.54	(22.32, 0.03, 0.94, 0.33)	(9.11, 0.21, −1.49)
Diffuse reflection model		
0.90	(22.38, 0.02, 0.95, 0.32)	(9.00, 0.22, −1.39)
Chromaticity		
1.61	(22.10, 0.04, 0.92, 0.30)	(8.90, −0.09, −1.46)

As we can see in Table 3 and in Fig. 9 (c), using chromaticity to establish matches between two range images of a specular object with different poses does not work. Indeed, the specular highlights are not removed, which tends to degrade the accuracy of matching. Similarly, the diffuse approximation performed worse than our proposed method. The specular reflections at the surface are ignored in the diffuse reflection model. In fact, we can observe in Fig. 9(b) that the specular highlights are present. This remainging specular highlights degraded the accuracy of matching. On the contrary, our proposed method successfully removed the specular highlights and, at the same time, estimated the albedo for almost all surface points. The obtained albedo image (see Fig. 9(a)) is thus reliable and accurate enough for matching points. The quantitative results also confirm the effectiveness of our proposed method.

6. Conclusion

We proposed a technique for extracting albedo of two range images of a specular object under fixed and uncontrolled illumination. By using highlights at the surface and illumination consistency on two range images, we estimate the incident illumination. We then use the illumination information and the dichromatic model of reflection in order to locally estimate albedo. Locally estimated albedo is then extrapolated into the whole surface to obtain reliable albedo. A range image registration technique is used to evaluate the usefulness of our proposed method. Experiments using synthetic data and real data confirm the robustness and the accuracy of our proposed method.

Acknowledgements

The authors are thankful to Robby T. Tan for his insightful suggestion on this work. This work was in part supported by JST, CREST.

References

[1] J.L Barron and D.J Fleet and S.S. Beauchemin, Performance of Optical Flow Techniques, *International Journal of Visual Computing*, vol. 12, o. 1, pp. 43–77, 1992.

[2] S. Biswas and G. Aggarwal and R. Chellapa, Robust Estimation of Albedo for Illumination-Invariant Matching and Shape Recovery, *IEEE Trans. on PAMI*, vol. 31, no. 5, pp. 884–899, 2009.

[3] N. Brusco and M. Andreetto and A. Giorgi and G. M. Cortelazzo, 3D registration by textured spin-images, *In Proc. of 3DIM'05*, pp. 262–269, 2005.

[4] L. Cerman and A. Sugimoto and I. Shimizu, 3D Shape registration with Estimating Illumination and photometric properties of a convex object, *In Proc. of CVWW'07*, pp. 76–81, 2007

[5] T.M Lehman and C. Palm, Color Line Search for Illuminant Estimation in Real-World Scene, *In J.Optics Soc.*,vol. 18, no. 11, pp. 2679–2691, 2001.

[6] S. Lin and T. Li and S.B. Kang and X. Tong and H.Y. Shum, Diffuse-Specular Separation and Depth Recovery from Image Sequences, *In Proc. of ECCV'02*, pp. 210–224, 2002.

[7] S.K. Nayar and X.S. Fang and T. Boult, Separation of Reflection Components Using Color and Polarization, *Int'l J. Computer Vision*, vol. 21, no. 3, 1996.

[8] S.K Nayar and K. Ikeuchi and T. Kanade, Surface Reflection: Physical and Geometrical Perspectives, *IEEE Trans. on PAMI*, vol. 13, no. 7, pp. 611–634, 1991.

[9] I.S. Okatani and A. Sugimoto, Registration of Range Images that Preserves Local Surface Structures and Color, *In Proc. of 3DPVT'04*, pp. 786–796, 2004

[10] K. Pulli and S. Piiroinen and T. Duchamp and W. Stuetzle, Projective Surface Matching of Colored 3D Scans, *In Proc. of 3DIM'05*, pp. 531–538, 2005.

[11] Y. Sato and K. Ikeuchi, Temporal-Color Space Analysis of Reflection, *J. Optics Soc. Am. A*, vol. 11, 1994.

[12] M. Shinozaki and M. Kusanagi and K. Umeda and G. Godin and M. Rioux, Correction of color information of a 3D model using range intensity image, *Computer Vision and Image Understanding*, vol. 113, no. 11, pp. 1170–1179, 2009.

[13] R.T. Tan and K. Ikeuchi, Separating Reflection Components of Textured Surfaces Using a Single Image, *IEEE Trans. on PAMI*, vol. 27, no. 2, pp. 178–193, 2005.

[14] R.T. Tan and K. Nishino and K. Ikeuchi, Color Constancy through Inverse Intensity Chromaticity Space, *J. Optics Soc. Am. A*, vol. 21, no. 3, pp. 321–334, 2004.

[15] D. Thomas and A. Sugimoto, Robust Range Image Registration using Local Distribution of Albedo, *In Proc. of 3DIM'09*, pp. 1654–1661, 2009.